Differentiation of Isomeric 1-, 3- and 7-Deazaadenosines by Electron Ionization Mass Spectrometry [a]

A. Mahender Reddy [b], Mark L. J. Reimer [c] and Karl H. Schram* [d]

Department of Pharmaceutical Sciences, College of Pharmacy, University of Arizona, Tucson, Arizona 85721 USA

Mario Grifantini and Gloria Cristalli

Institute of Pharmaceutical and Organic Chemistry, University of Camerino, 62032 Camerino (MC), Italy

Received October 10, 1989

The low and high resolution electron ionization mass spectra of 1-deazaadenosine, 3-deazaadenosine and 7-deazaadenosine are reported. Fragmentation pathways and ion structures are proposed with the aid of linked-scan, daughter-ion spectra. Results indicate that the N-3 position of the purine ring serves as an important acceptor site in fragmentation processes involving hydrogen transfer from the sugar to the base. A mixture analysis of the trimethylsilyl derivatives of adenosine, 1-, 3- and 7-deazaadenosine by combined gas chromatography/mass spectrometry is also described.

J. Heterocyclic Chem., **27**, 1297 (1990).

Introduction.

Establishing correlations between molecular structure and biological activity has long been a research priority among medicinal chemists and pharmaceutical scientists. Recent studies of the modified nucleosides 1-deazaadenosine (**1**), 3-deazaadenosine (**2**) and 7-deazaadenosine (**3** have focused on their ability to inhibit both blood platelet aggregation [1] and adenosine deaminase [2]. This isomeric set has also been examined for its adenosine receptor affinity in radioligand binding studies [3], with the relative contributions of purine nitrogen atoms to binding at A_1 rat brain adenosine receptors decreasing in the order N-7 > N-3 > N-1. 1-Deazaadenosine has exhibited good *in vitro* cytotoxicity towards two human cell lines (HeLa and KB) and three murine leukemia cell lines (P388, P388 doxorubicin resistant, and L1210) when compared with the antineoplastic agents 5-fluorouracil (5-FU), 1-β-D-arabinofuranosylcytosine (ara-C) and 1-β-D-arabinofuranosyladenine (ara-A) [4]. 7-Deazaadenosine (tubercidin) is a potent antitumor antibiotic known to inhibit DNA-dependent RNA polymerases in the cell [5].

One of the major applications of mass spectrometry in the field of nucleic acid chemistry has been the identification of modified nucleosides isolated from biological sources such as human urine [6-10]. Structural elucidation of these compounds has generally depended upon low and high resolution electron ionization (EI) analyses, primarily because of the abundant fragment ion information obtained, but also because of the well-documented structure-fragmentation relationships established for both free [11] and trimethylsilyl-derivatized (TMS) nucleosides [11-13]. However, recent reports [14,15] indicate that minor modifications in nucleoside structure can result in mass spectra which deviate considerably from predictions based upon standard purine or pyrimidine skeletons. The availability of the isomeric mono-deazaadenosines **1-3** affords a unique opportunity to evaluate the influence of the various nitrogen atoms on the fragmentation patterns of purine nucleosides. Such a study can be of considerable value in distinguishing between possible ion intermediates and fragmentation mechanisms in the mass spectrometry of this important compound class.

The structures and molecular weights of compounds **1-3** and adenosine (**4**) are given in Table 1, as are their TMS derivatives **5-8**. Normal EI magnetic sector scans and linked-scan spectra (the latter with collisional activation [CA]) were acquired for **1-4**. Structures and fragmentation pathways are proposed for those ions characteristic of each of the isomers. Results indicate that the N-3 position

Table 1

Names, Structures and Molecular Weights of Compounds Examined

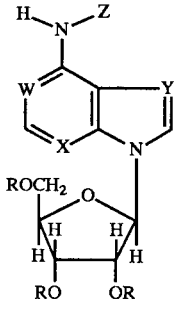

	Compound	W	X	Y	Z	R	MW
1	1-Deazaadenosine	CH	N	N	H	H	266
2	3-Deazaadenosine	N	CH	N	H	H	266
3	7-Deazaadenosine	N	N	CH	H	H	266
4	Adenosine	N	N	N	H	H	267
5	1-Deazaadenosine-$(TMS)_4$	CH	N	N	TMS	TMS	554
6	3-Deazaadenosine-$(TMS)_4$	N	CH	N	TMS	TMS	554
7	7-Deazaadenosine-$(TMS)_4$	N	N	CH	TMS	TMS	554
8	Adenosine-$(TMS)_4$	N	N	N	TMS	TMS	555

of the purine ring serves as an important acceptor site in fragmentation processes involving hydrogen transfer from the sugar to the base. Finally, a mixture analysis of compounds **5-8** was performed by EI gas chromatography/mass spectrometry (gc/ms), demonstrating the power of this technique for the separation and identification of nucleoside mixtures.

EXPERIMENTAL

Samples.

Adenosine and 7-deazaadenosine were purchased from Sigma Chemical (St. Louis, MO). The syntheses of 1-deazaadenosine and 3-deazaadenosine have been previously described [4,16,17].

Materials.

N,O-Bis(trimethylsilyl)trifluoroacetamide (BSTFA) containing 1% trimethylchlorosilane (TMCS) was purchased from Pierce Chemical Co., Rockford, IL. Other reagents and hplc-grade solvents were purchased from commercial sources and used without further purification.

Derivatization.

Trimethylsilyl derivatives **5-8** were prepared [18] by heating each nucleoside (10 μg) in a 50 μL solution of BSTFA/TMCS and

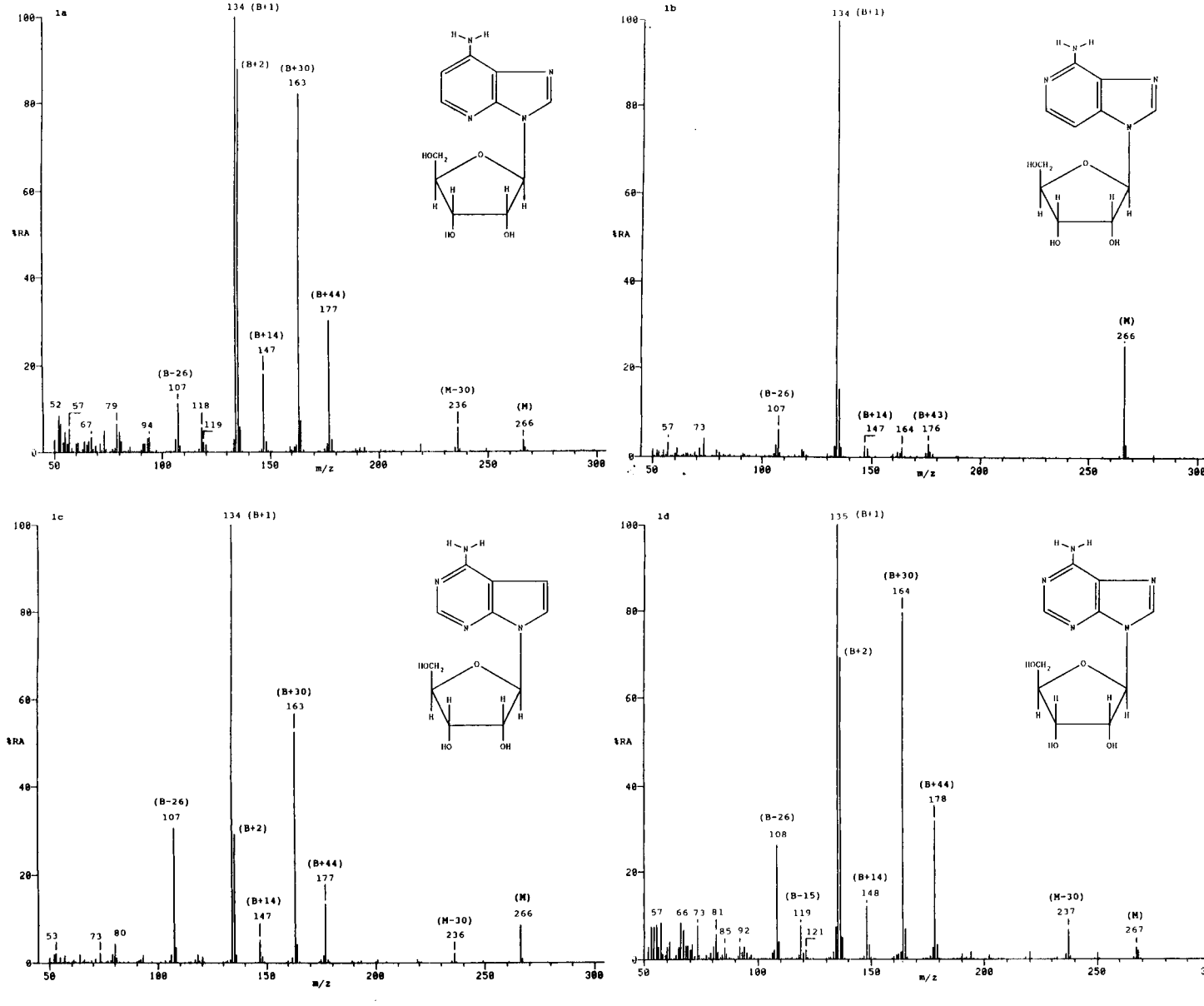

Figure 1. Low resolution EI mass spectra of (a) 1-deazaadenosine, **1**; (b) 3-deazaadenosine, **2**; (c) 7-deazaadenosine, **3**; and (d) adenosine, **4**.

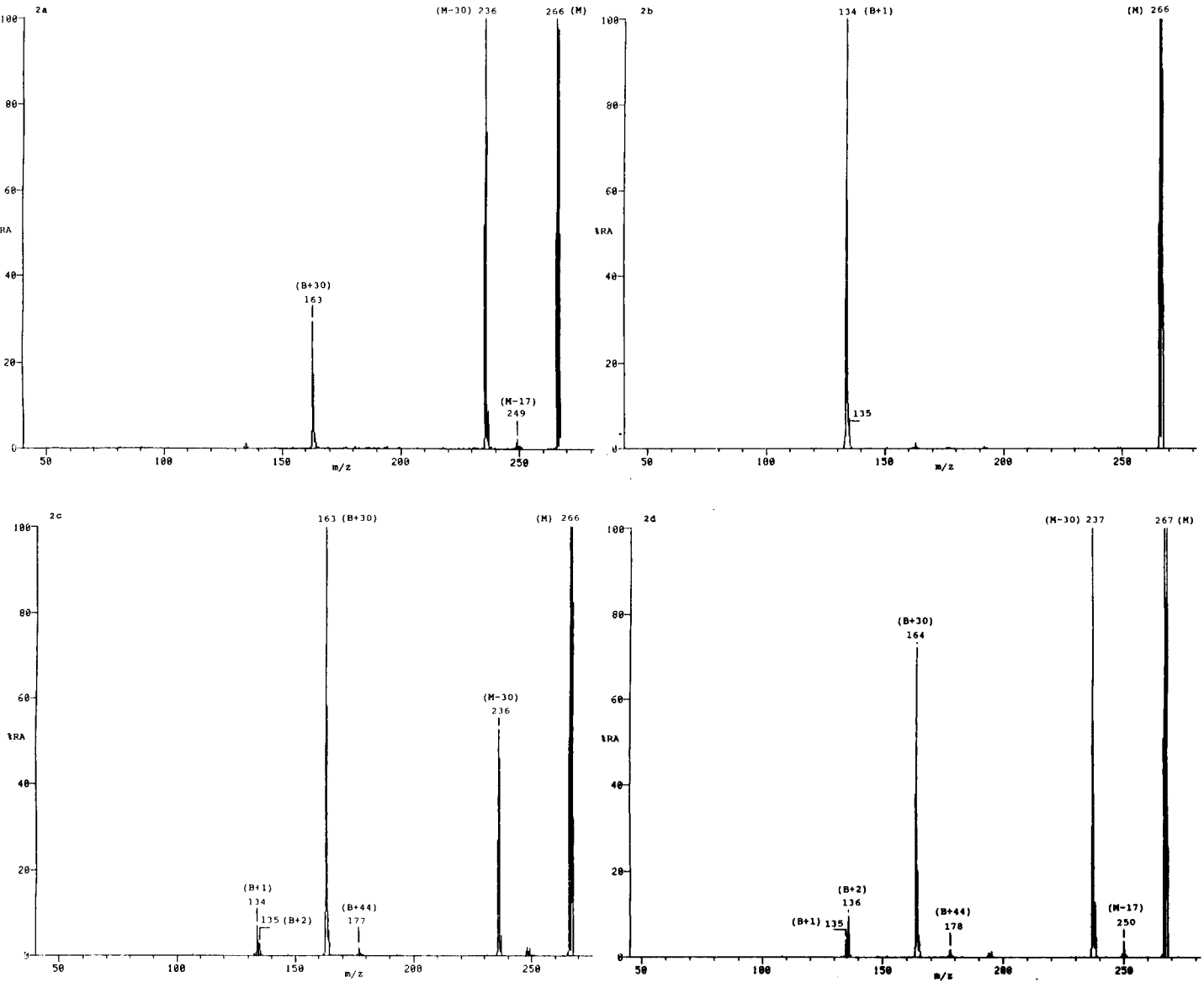

Figure 2. CA linked-scan daughter-ion spectra of $[M]^{+\cdot}$ of (a) 1-deazaadenosine, **1**; (b) 3-deazaadenosine, **2**; (c) 7-deazaadenosine, **3**; and (d) adenosine, **4**.

pyridine (80:20) for one hour at 100°.

Mass Spectrometry.

All mass spectra were acquired on a Finnigan MAT 90 double-focusing (BE) instrument (Finnigan MAT, San Jose, CA); system control, data acquisition and processing were carried out by an integrated multi-processor system based on a Micro VIP 11/73 computer (U.S. Design, Lanham, MD).

Compounds **1-4** were introduced by direct insertion probe for all standard EI and linked scan spectra. The low resolution mass spectrometry conditions were as follows: ionizing energy, 70 eV; emission current, 1.0 mA; source temperature, 250°; scan rate, 1.0 sec/decade; scan range, m/z 45 to 450; resolution, 1000 (10% valley definition). High resolution mass measurements were carried out under similar conditions at a scan rate of 5.0 sec/decade and a resolution of 7500.

Linked scans at constant magnetic field/electric field ratio (B/E; accelerating voltage (V) constant) were obtained on $[M]^{+\cdot}$ and selected fragment ions of **1-4** at a scan rate of 5.0 sec/decade. Collisional activation analyses were achieved in the first field-free region (FFR) of the instrument by adjusting the argon pressure in the collision cell so that approximately 50% attenuation of the $[M]^{+\cdot}$ signal was achieved.

The gc/ms analyses of compounds **5-8** were performed using a Varian Model 3400 gas chromatograph directly coupled to the MAT 90. Sample introduction was *via* splitless injection onto a fused silica DB-5 capillary column (30 m x 0.25 mm; 0.25 μm film thickness; J & W Scientific, Folsom, CA). The following gc conditions were used: initial column temperature, 150°; program rate, 6°/minute; final column temperature, 300° (held for 10 minutes);

helium carrier gas at a head pressure of 10 psi; injector port and transfer line temperatures, 300°. One μl of compounds **5-8** were used to prepare the nucleoside mixture. The sample injection volume was 1.0 μl. The EI analyses were performed under the low resolution conditions described above, with the exception that a 0.4 second/decade scan rate was used over a scan range of m/z 70 to 1000.

Results and Discussion.

Free Compounds.

The low resolution EI mass spectra of **1-4** are shown in Figure 1 while the corresponding B/E daughter scans of $[M]^{+\cdot}$ are depicted in Figure 2.

Ions (and ion pairs) which appear useful in differentiating between isomers include: $[M]^{+\cdot}$, $[M-30]^{+\cdot}$, $[B+44]^{+}/[B+43]^{+\cdot}$, $[B+30]^{+}$, $[B+14]^{+}$, $[B+2]^{+}/[B+1]^{+\cdot}$ and $[B-26]^{+}$. Where necessary, the significance, structure and mechanism of formation of these ions are discussed. Elemental compositions of all significant ions present in the high resolution mass spectra of **1-3** are given in Table 2 (adenosine is included in this study primarily for comparative purposes as its mass spectrum has been studied in detail [11,19]).

Table 2
Elemental Composition and Structural Assignment of Significant Ions in the High Resolution Mass Spectra of Compounds 1, 2 and 3

	m/z (observed)	Error (mnu) [a]	Composition	Assignment [b]
1	266.0994	+2.1	$C_{11}H_{14}N_4O_4$	$[M]^{+\cdot}$
2	266.1034	-1.9		
3	266.0998	+1.7		
1	249.1024	-3.6	$C_{11}H_{13}N_4O_3$	$[M-17]^{+}$
2	--	--		
3	249.0979	+1.0		
1	236.0994	-2.1	$C_{10}H_{12}N_4O_3$	$[M-30]^{+\cdot}$
2	--	--		
3	236.0883	+2.7		
1	193.0678	+4.8	$C_8H_9N_4O_2$	$[B+60]^{+}$
2	--	--		
3	193.0719	+0.6		
1	177.0765	+1.1	$C_8H_9N_4O$	$[B+44]^{+}$
2	177.0763	+1.3		
3	177.0768	+0.9		
1	--	--		
2	176.0699	+0.1	$C_8H_8N_4O$	$[B+43]^{+\cdot}$
3	--	--		
1	163.0607	+1.3	$C_7H_7N_4O$	$[B+30]^{+}$
2	163.0595	+2.5		
3	163.0601	+1.9		
1	147.0641	+3.0	$C_7H_7N_4$	$[B+14]^{+}$
2	147.0638	+3.2		
3	147.0653	+1.8		
1	135.0638	+3.2	$C_6H_7N_4$	$[B+2]^{+}$
2	135.0617	+5.4		
3	135.0638	+3.2		
1	134.0571	+2.1	$C_6H_6N_4$	$[B+1]^{+\cdot}$
2	134.0568	+2.4		
3	134.0564	+2.9		
1	118.0407	-0.2	$C_6H_4N_3$	$[B-15]^{+\cdot}$
2	118.0407	-0.2		
3	118.0422	-1.7		
1	107.0467	+1.6	$C_5H_5N_3$	$[B-26]^{+}$
2	107.0472	+1.2		
3	107.0466	+1.7		

[a] Error = calculated mass - observed mass; mmu = millimass units.
[b] A more detailed structural assignment is given in the text.

$[M]^{+\cdot}$.

A molecular ion is seen in each of the spectra (m/z 266 in **1-3**, m/z 267 in **4**), although the relative abundance of $[M]^{+\cdot}$ clearly decreases in the order **2** > **3** > **1** ≈ **4**. This trend is reflected in the decreased fragmentation (enhanced stability) of 3-deazaadenosine as compared to **1**, **3** and **4**. The daughter ion spectra of $[M]^{+\cdot}$ (Figure 2) support this observation: several intense metastable transitions are evident in **1**, **3** and **4**, while **2** exhibits only a single transition (m/z 266 → m/z 134, $[B+1]^{+\cdot}$).

$[M-30]^{+\cdot}$.

The loss of 30 daltons (Da) (CH_2O) from the molecular ion of a nucleoside is considered a strong indicator of a 5′-hydroxyl functionality [11,19]. Two pathways have been proposed for the formation of $[M-30]^{+\cdot}$:

Structure Set #1

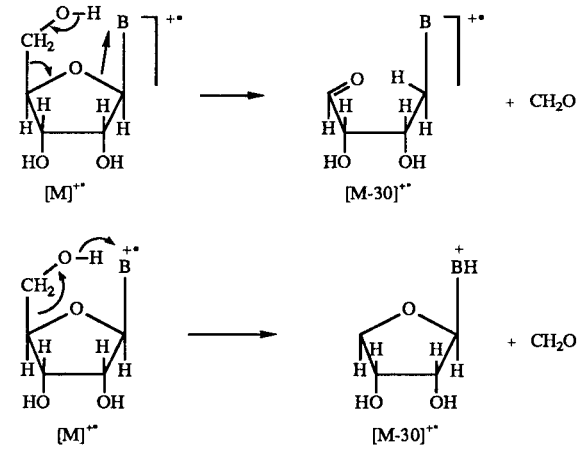

The first mechanism [20] involves transfer of the 5′-hydroxyl hydrogen to C-1′, a process which would appear to be relatively independent of modifications in the base, with the possible exception of minor electronic effects. The second mechanism requires transfer of the 5′-hydroxyl hydrogen to some position on the charge-localized base, which model studies have shown to be possible when the molecule adopts a sterically-accessible *syn* conformation [19]. The utility of the latter mechanism is also conditional upon the availability of a hydrogen "acceptor" on the aglycone. A comparison of the spectra in Figure 1 gives some insight into the possible fragmentation mechanism at work. The spectrum of 3-deazaadenosine (Figure 1(b)) shows the complete absence of $[M-30]^{+\cdot}$, thus lending support to the second mechanism while simultaneously suggesting that N-3 is an important site for accepting the transferred hydrogen. The N-1 and N-7 positions in the purine heterocycle do not appear to be as important as N-3 for hydrogen transfer; $[M-30]^{+\cdot}$ has measureable abundance in both **1** (m/z 236, 5.5%) and **3** (m/z 236, 2.1%), although both are slightly diminished as compared to adenosine (m/z 237, 6.9%).

$[B+44]^+/[B+43]^{+\cdot}$.

A major ion in the mass spectra of purine ribosides occurs at 44 Da above the mass of the base; this ion is observed in **1** (m/z 177, 30.2%), **3** (m/z 177, 13.5%) and **4** (m/z 178, 31.6%), but is nearly absent in the mass spectrum of **2** (m/z 177, 1.4%). One possible pathway for the formation of $[B+44]^+$ is analogous to the formation of $[B+116]^+$ in TMS-derivatized nucleosides [13] and involves opening of the sugar ring, transfer of H-4′ to the base and cleavage of the C-1′/O-4′ bond:

Structure Set #2

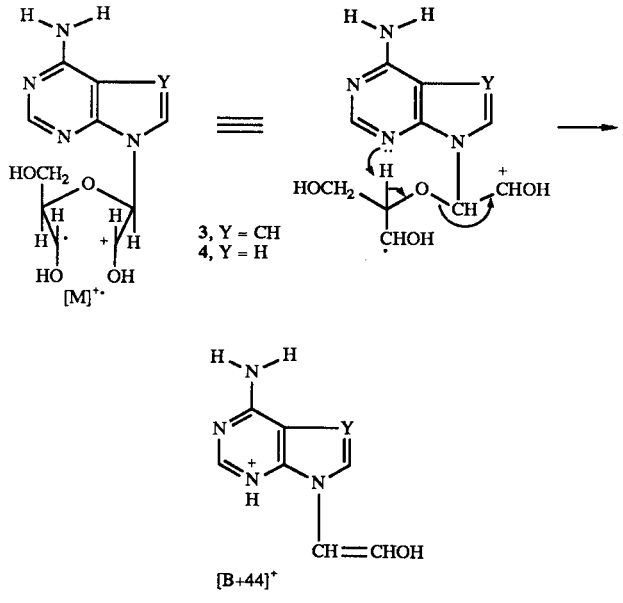

However, linked-scan results on $[M]^{+\cdot}$ (Figure 2) show that the corresponding metastable transition ($[M]^{+\cdot} \rightarrow [B+44]^+$) is only present in **3** and **4**. While the absence of $[B+44]^+$ in **2** is predictable based on the importance of N-3 as a hydrogen-accepting site, the above mechanism does not adequately explain the lack of an appropriate metastable transition in the $[M]^{+\cdot}$ daughter ion spectrum of **1** (Figure 2(a)). Additional linked-scanning experiments (spectra not shown) revealed that $[M-30]^{+\cdot}$ is a possible precursor of $[B+44]^+$ in **1**, **3** and **4**:

Structure Set #3

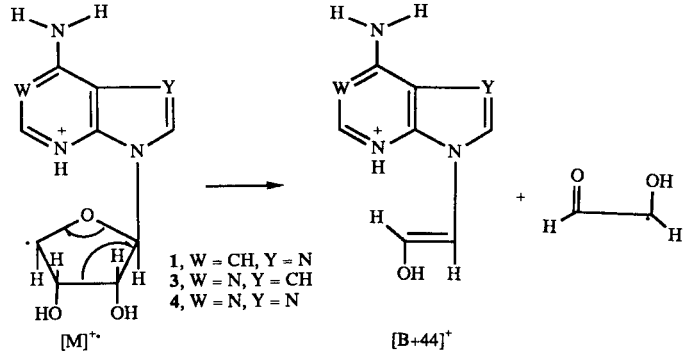

Having $[M-30]^{+\cdot}$ as a precursor accounts for the prominence of $[B+44]^+$ in **1**, **3** and **4** (all of which have a weakly-to-moderately abundant $[M-30]^{+\cdot}$) and its relative absence in **2**. A minor peak at m/z 176 in **2** ($[B+43]^{+\cdot}$, see Table 2) appears characteristic of the 3-deaza isomer and may be the result of hydrogen transfer from O-2′ to C-1′ concomitant with cleavage of the sugar ring:

Structure Set #4

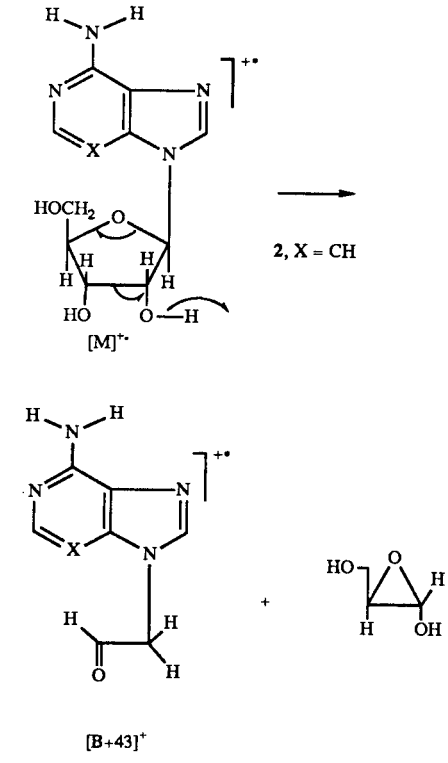

Although strong metastable evidence is lacking for this process, the 3-deaza purine moiety's inability to compete for the transfered hydrogen (to form $[B+44]^+$) provides a possible rationale.

$[B+30]^+$.

The abundance of $[B+30]^+$ serves as another strong indicator of the importance of N-3 in the fragmentation of adenosine and mono-deazaadenosines. A major ion in the spectra of **1** (m/z 163, 82.3%), **3** (m/z 163, 52.7%) and **4** (m/z 164, 79.5%), $[B+30]^+$ is absent in **2**. Consisting of the base, C-1′, the sugar ether oxygen and two hydrogens, $[B+30]^+$ has been considered structurally diagnostic of a free 2′-hydroxyl group [19], yet present results suggest that the availability of the N-3 position (when the purine heterocycle is in an *anti* configuration) plays a significant role in the overall mechanism:

Structure Set #5

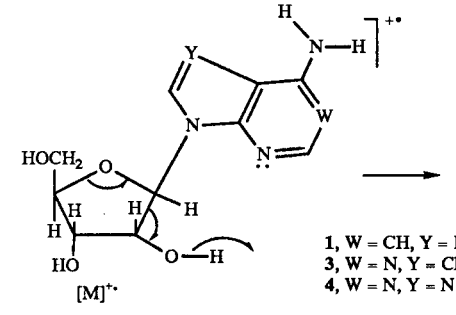

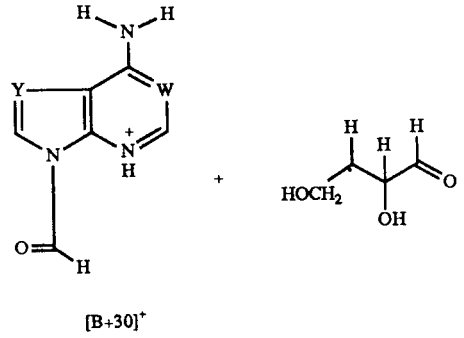

[B+30]$^+$

Metastable data (Figure 2) confirm the $[M]^{+\cdot} \rightarrow [B+30]^+$ transition in **1**, **3** and **4**.

$[B+14]^+$.

A moderately-intense peak in the spectra of **1** (m/z 147, 18.1%), **2** (m/z 147, 3.1%), **3** (m/z 147, 5.3%) and **4** (m/z 148, 12.1%), $[B+14]^+$ is of interest because of the different mechanisms responsible for its formation. Metastable evidence (spectra not shown) indicates that $[B+14]^+$ is formed *via* the loss of CH_2O from $[B+44]^+$ in **1**, **3** and **4**:

Structure Set #6

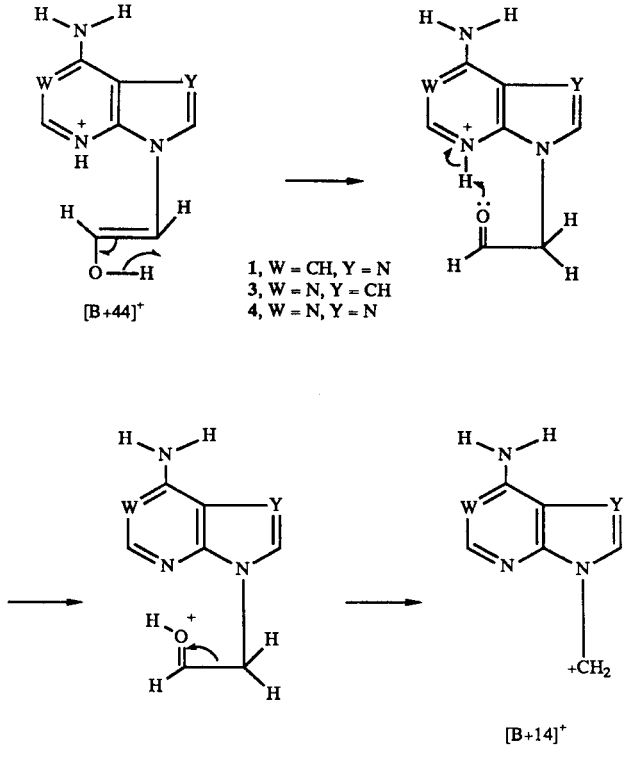

[B+44]$^+$

[B+14]$^+$

However, as **2** lacks an appreciable $[B+44]^+$ abundance, $[B+14]^+$ is also believed to arise through the inductive elimination of $HCO^{\cdot}$ from the odd-electron species $[B+43]^{+\cdot}$ (m/z 176):

Structure Set #7

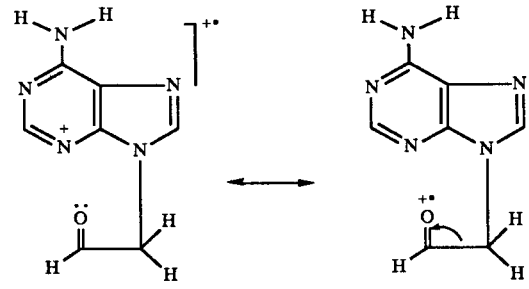

2, $[B+43]^{+\cdot}$

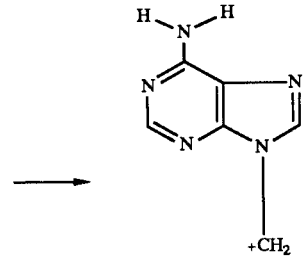

[B+14]$^+$

$[B+2]^+/[B+1]^{+\cdot}$.

The base peak in all of the spectra is $[B+1]^{+\cdot}$, formed from $[M]^{+\cdot}$ by cleavage of the glycosidic bond and transfer of a hydroxyl hydrogen from the sugar to the base [11] (a mechanism supported by the $[M]^{+\cdot}$ daughter ion spectra in Figure 2). Hydrogen attachment does not appear to be as "site specific" in $[B+1]^{+\cdot}$ as

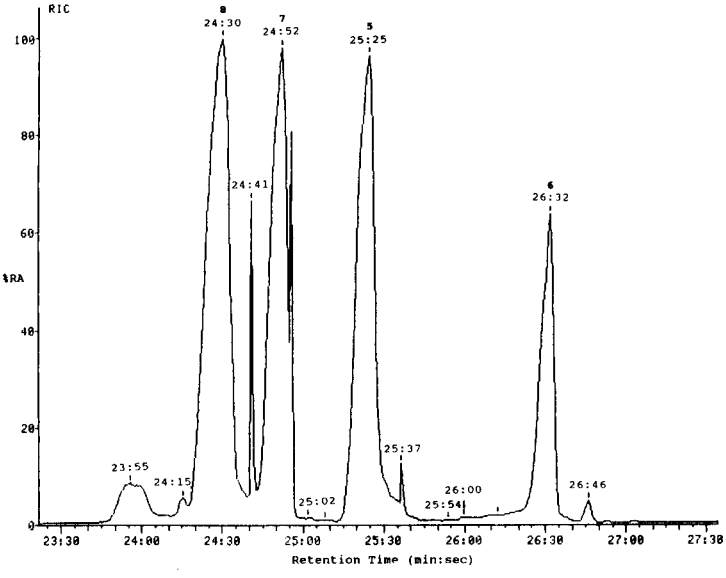

Figure 3. Reconstructed ion chromatogram for the nucleoside mixture **5-8**.

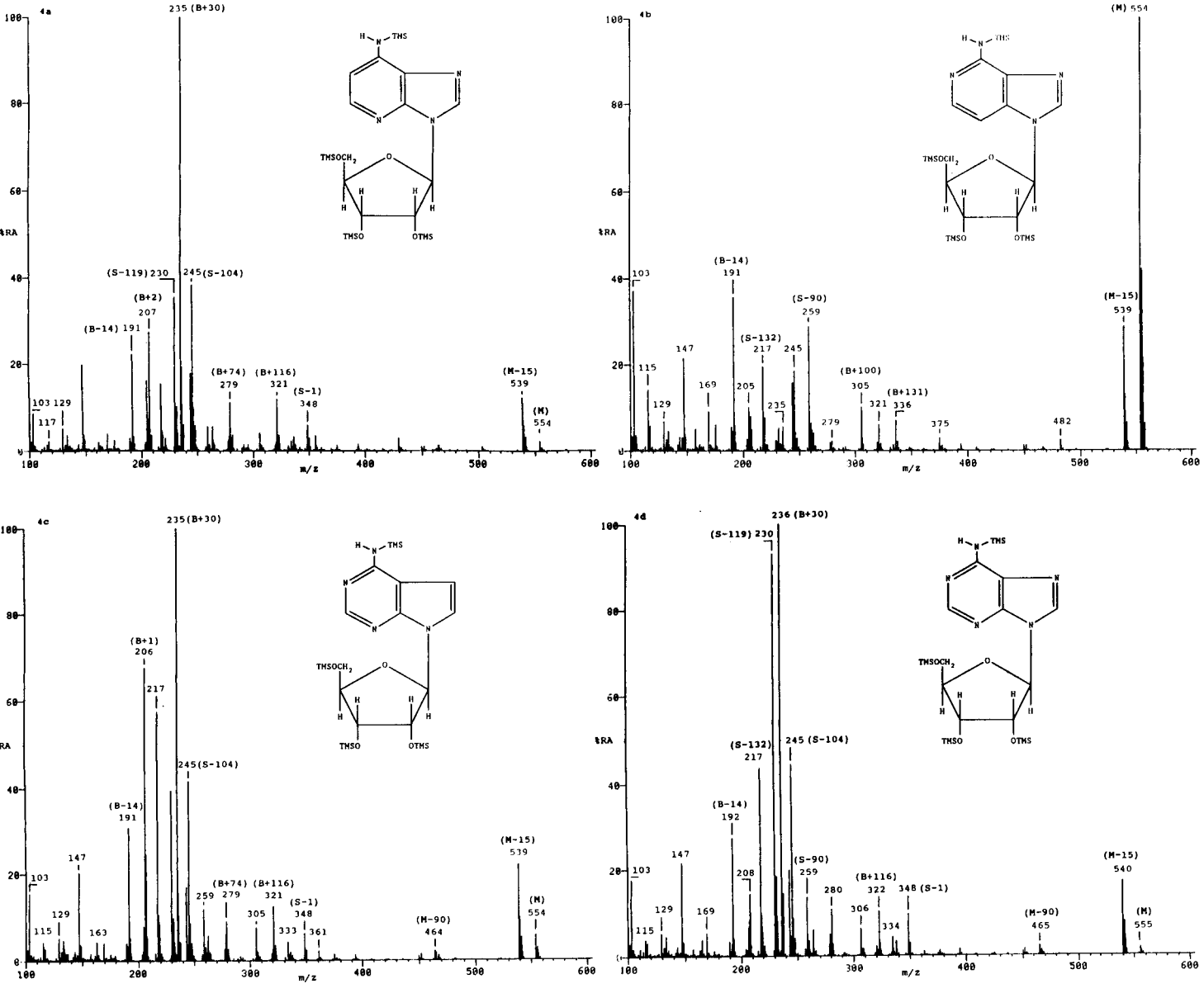

Figure 4. Low resolution EI mass spectra of (a) 1-deazaadenosine-(TMS)$_4$, **5**; (b) 3-deazaadenosine-(TMS)$_4$, **6**; (c) 7-deazaadenosine-(TMS)$_4$, **7**; and (d) adenosine-(TMS)$_4$, **8**.

it is in other ions of this mono-deaza series; $[B+1]^{+\cdot}$ forms the base peak in all four compounds, including 3-deazaadenosine. On the other hand, the abundances of $[B+2]^+$ (base plus two transferred hydrogens) vary widely, from 14.0% in **2** and 29.0% in **3** to 69.2% in **4** and 88.1% in **1**. While formation of $[B+2]^+$ from $[M]^{+\cdot}$ is indicated as a minor metastable process for **1-4**, an alternative pathway to $[B+2]^+$ may be *via* the loss of CO from $[B+30]^+$:

Sturcture Set #8

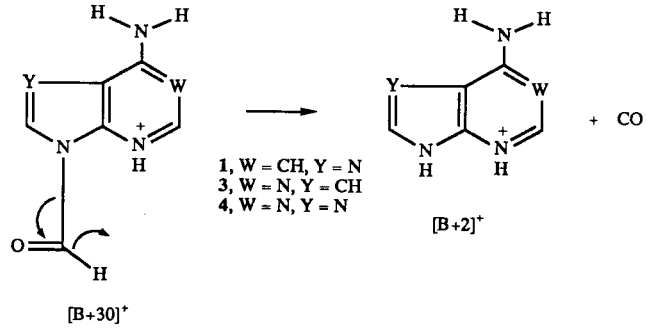

Daughter-ion experiments (spectra not shown) confirm that $[B+30]^+$ is indeed a precursor of $[B+2]^+$ for **1**, **3** and **4**. This relationship explains the variable abundances observed for $[B+2]^+$: since $[B+30]^+$ formation is not favored in **2**, the $[B+30]^+ \rightarrow [B+2]^+$ pathway is restricted and $[B+2]^+$ abundance is reduced. Conversely, significant $[B+30]^+$ intensities are seen in **1**, **3** and **4**, thereby leading to greater opportunities for $[B+2]^+$ generation.

$[B-26]^+$.

The loss of a molecule of HCN from $[B+1]^{+\cdot}$ is an established fragmentation in adenosine and related analogs [19]. Deuterium labeling studies [21] indicate that the required elements originate almost equally from C-6/N-6 and from C-2 and either N-1 or N-3. On this basis, $[B-26]^+$ ion abundances should be greatest in **3** and **4** (each possessing both N-1 and N-3) and smallest in **1** and **2**. These predictions are verified in the EI mass spectra of Figure 1: **1** (m/z 107, 11.3%), **2** (m/z 107, 6.2%), **3** (m/z 107, 30.5%) and **4** (m/z 108, 26.2%).

GC/MS Analysis of TMS Derivatives.

The reconstructed ion chromatogram (RIC) for the nucleoside mixture **5-8** is given in Figure 3 (only the region containing the four nucleosides is shown).

The elution order and retention times (minutes:seconds) for the gc/ms profile were: **8** (24.30), **7** (24.52), **5** (25:25) and **6** (26.32). Small satellite peaks in the RIC are due to incomplete derivatization and/or background; an unresolved mixture of $(TMS)_3$ and $(TMS)_4$ derivatives of **6** appear from 26:00 to 26:23 minutes perhaps accounting for the diminished intensity of **6** as compared to the other peaks. The RIC represents an on-column injection of approximately 50 ng of each nucleoside.

The mass spectra of **5-8** are shown in Figure 4. All spectra are normalized to the most abundant ion above m/z 100. As with other mass spectral investigations involving trimethylsilylated nucleosides [12,13], the major fragment ions are derived from either (i) the molecular ion, $[M]^{+\cdot}$, (ii) the intact base plus a proton of the sugar (S), or (iii) the sugar.

Molecular Ion-Related Species.

The abundance of $[M]^{+\cdot}$ is uniformly low in **5** (m/z 554, 2.1%), **7** (m/z 554, 5.9%) and **8** (m/z 555, 1.7%), yet this ion is the base peak in the spectrum of **6** (m/z 554, 100%). The molecular ion stabilities of the TMS derivatives essentially parallel the trend established earlier for the free compounds; the extraordinary lifetime of $[M]^{+\cdot}$ in 3-deazaadenosine-$(TMS)_4$ results in a spectrum displaying minimal fragmentation, while the greater fragmentation in **5**, **7** and **8** is reflected in diminished $[M]^{+\cdot}$ intensities. All compounds exhibit $[M-15]^+$ (loss of a methyl radical), while peaks due to $[M-90]^{+\cdot}$ (loss of TMSOH), $[M-103]^+$ (elimination of CH_2OTMS from 5′ position) and $[M-105]^+$ (loss of TMSOH from $[M-15]^+$) appear in most spectra.

Base-Related Ions.

The most striking feature of this ion series is that $[B+30]^+$ constitutes the most intense peak in **5** (m/z 235, 100%), **7** (m/z 235, 100%) and **8** (m/z 236, 100%), but is nearly absent by comparison in **6** (m/z 235, 5.7%). Once again, hydrogen rearrangement from the sugar to the base (a requirement in the proposed mechanisms [12,13] leading to $[B+30]^+$) is hindered considerably in 3-deazaadenosine, reemphasizing the importance of N-3 as a site for attachment of the transferred hydrogen. An interesting trend is seen when the ratio of $[B+116]^+/[B+100]^+$ and $[B+74]^+/[B+58]^+$ abundances are compared among **5-8**. $[B+100]^+$ is believed to be derived from $[B+116]^+$ by the elimination of a rearranged hydrogen and a silyl methyl group; a similar relationship applies to $[B+58]^+$ and $[B+74]^+$. Examining the spectra in Figure 4, the $[B+116]^+/[B+100]^+$ and $[B+74]^+/[B+58]^+$ ratios are all greater than one in **5**, **7** and **8**, whereas they are considerably less than one in **6**. These empirical observations suggest that some measure of added stability may be afforded ions possessing a rearranged hydrogen ($[B+116]^+$ and $[B+74]^+$) if they also have an available N-3 position (as in **5**, **7** and **8**) to act as a site for hydrogen attachment.

Sugar-Related Ions.

The major differences in sugar ion abundances are associated with 3-deazaadenosine-$(TMS)_4$, where once again the absence of N-3 affects normal fragmentation patterns. Sugar ions that are missing or suppressed in the mass spectrum of **6** (Figure 4 (b)) include $[S-1]^{+\cdot}$ ($[S-H]^{+\cdot}$, m/z 348) and $[S-119]^{+\cdot}$ ($[C_4H_4O_2(TMS)_2]^{+\cdot}$, m/z 230). Since hydrogen transfer to the base is required for its formation, a low $[S-1]^{+\cdot}$ abundance in **6** is not unexpected. Although the mechanism for the formation of $[S-119]^{+\cdot}$ is not well understood [12], present evidence implies that the N-3 position plays a critical role in the process.

Conclusions.

The mass spectral comparison of 1-, 3- and 7-deazaadenosine establishes the dominance of the N-3 position in directing purine nucleoside fragmentation processes. A key aspect in the mechanisms of formation of $[M-30]^+$, $[B+44]^+$ and $[B+30]^+$, the transfer of a hydrogen from the sugar to the aglycone is significantly diminished in **2** versus **1** and **3** as evidenced by the reduced abundances of these ions in the mass spectrum of 3-deazaadenosine. The close proximity of the unshared electron pair on N-3 to either the ring hydrogens or hydroxyl hydrogens on the sugar would appear to be the basis for this important interaction. While distinguishing 3-deazaadenosine from 1- and 7-deaza isomers is straight-forward, the differentiation of 1-deazaadenosine from 7-deazaadenosine is less obvious and relies primarily upon differences in $[M-30]^+$, $[B+2]^+$ and $[B-26]^+$ abundances. From the standpoint of overall influence on fragmentation behavior (as compared to adenosine), the order N-3 > N-7 > N-1 applies.

Acknowledgments.

The authors thank Mr. Peter F. Baker and Mr. Kurt L. Kennedy for their assistance in the operation and maintenance of the mass spectrometer. This work was supported by a National Institutes of Health grant (CA43068) awarded to K. H. S.

REFERENCES AND NOTES

[a] A preliminary account of this work was presented at the Fourth National Symposium on Mass Spectrometry, Indian Institute of Science, Bangalore, India, January 4-6, 1988.

[b] Present address: Lederle Laboratories, American Cyanamid, Pearl River, New York.

[c] Present address: Biomedical Mass Spectrometry Unit, McGill University, Montreal, Quebec, Canada.

[d] Author to whom correspondence should be addressed.

[1] I. Antonini, G. Cristalli, P. Franchetti, M. Grifantini, S. Martelli

and F. Petrelli, *J. Pharm. Sci.*, **73**, 366 (1984).

[2] G. Lupidi, F. Riva, G. Cristalli and M. Grifantini, *Ital. J. Biochem.*, **31**, 396 (1982).

[3] G. Cristalli, M. Grifantini, S. Vittori, W. Balduini and F. Cattabeni, *Nucleosides Nucleotides*, **4**, 625 (1985).

[4] G. Cristalli, P. Franchetti, M. Grifantini, S. Vittori, T. Bordoni and C. Geroni, *J. Med. Chem.*, **30**, 1686 (1987).

[5] W. E. G. Muller in Nucleoside Analogues, R. T. Walker, E. De Clerq and F. Eckstein, eds, Nato Advanced Study Institutes Series, Vol **26**, Plenum Press, New York, 1979, p 247.

[6] G. B. Chheda, H. B. Patrzyc, A. K. Bhargava, P. F. Crain, S. K. Sethi, J. A. McCloskey and S. P. Dutta, *Nucleosides Nucleotides*, **6**, 597 (1987).

[7] G. B. Chheda, H. A. Tworek, A. K. Bhargava, E. Rachlin, S. P. Dutta and H. B. Patrzyc, *Nucleosides Nucleotides*, **7**, 417 (1988).

[8] T. D. McClure, K. H. Schram, K. Nakano and T. Yasaka, *Nucleosides Nucleotides*, **8**, 1399 (1989).

[9] T. D. McClure, K. H. Schram, K. Nakano and T. Yasaka, *Nucleosides Nucleotides*, **8**, 1417 (1989).

[10] M. L. J. Reimer, K. H. Schram, K. Nakano and T. Yasaka, *Anal. Biochem.*, **181**, 302 (1989).

[11] J. A. McCloskey in Basic Principles in Nucleic Acid Chemistry, Vol **1**, P. O. P. Ts'o, ed, Academic Press, New York, 1974, p 209.

[12] H. Pang, K. H. Schram, D. L. Smith, S. P. Gupta, L. B. Townsend and J. A. McCloskey, *J. Org. Chem.*, **47**, 3923 (1982).

[13] M. L. J. Reimer, T. D. McClure and K. H. Schram, *Biomed. Environ. Mass Spectrom.*, **18**, 533 (1989).

[14] K. H. Schram and D. Prince, *Biomed. Mass Spectrom.*, **10**, 34 (1983).

[15] E. M. Schubert, K. H. Schram and R. A. Glennon, *J. Heterocyclic Chem.*, **22**, 889 (1985).

[16] G. Cristalli, P. Franchetti, M. Grifantini, S. Vittori, T. Bordoni and C. Geroni, *Nucleosides Nucleotides*, **6**, 381 (1987).

[17] J. A. Montgomery, A. T. Shortnacy and S. D. Clayton, *Biochem. Pharmacol.*, **14**, 195 (1977).

[18] K. H. Schram and J. A. McCloskey in GLC and HPLC Determination of Therapeutic Agents, K. Tsuji, ed, Part **3**, Dekker, New York, 1979, p 1149.

[19] S. J. Shaw, D. M. Desiderio, K. Tsuboyama and J. A. McCloskey, *J. Am. Chem. Soc.*, **92**, 2510 (1970).

[20] K. Biemann and J. A. McCloskey, *J. Am. Chem. Soc.*, **84**, 2005 (1962).

[21] J. L. Occolowitz, *Chem. Commun.*, 1226 (1968).